Inorganic Chemistry
Article

Inorg. Chem. **2009**, *48*, 5073–5080 **5073**
DOI: 10.1021/ic8023524

A Family of Polynuclear Clusters Containing Cyano-Bridged T-Shaped $Fe_3^{III}M^{II}$ (M = Cu, Co, Mn) Metal Cores: Syntheses, Structures, and Magnetic Properties

Zhi-Guo Gu, Yi-Fan Xu, Ling-Chen Kang, Yi-Zhi Li, Jing-Lin Zuo,* and Xiao-Zeng You

State Key Laboratory of Coordination Chemistry, School of Chemistry and Chemical Engineering, Nanjing National Laboratory of Microstructures, Nanjing University, Nanjing 210093, P. R. China

Received December 9, 2008

A new family of polynuclear clusters containing the $Fe_3^{III}M^{II}$ cores $[(Tp^{4Bo})_6Fe_6(CN)_{18}M_2Na_2(H_2O)_{16}]\cdot 4H_2O$ (M = Cu, Co, Mn; **1**−**3**) and $[(Tp^{4Bo})_6Fe_6(CN)_{18}M_2Na_2(H_2O)_{12}(DMF)_4]\cdot H_2O$ (M = Cu, Co, Mn; **4**−**6**) have been synthesized and structurally characterized. Complexes **1**−**3** crystallize in the $P2_1/c$ space group, and **4**−**6** crystallize in the $P2_1/n$ space group. All six complexes consist of two symmetry-related T-shaped $[(Tp^{4Bo})_3(CN)_9Fe_3M]^-$ subunits linked by two Na^+ cations. Each polynuclear cluster in **1**−**6** strongly interacts with 12 adjacent such units through $\pi-\pi$ interactions, leading to the formation of 3D 12-connected frameworks. Magnetic studies show appreciable magnetic anisotropies in compounds **1**, **2**, **4**, and **5**. Antiferromagnetic interactions were observed in complexes **3** and **6**.

Introduction

Single-molecule magnets (SMMs) have attracted much interest over the past 10 years, not only from the scientific point of view on quantum tunneling of magnetization and quantum phase interference but also because of their potential applications in high-density magnetic storage, quantum computing, and more recently of spintronics.[1,2] The requirement of a SMM is the combination of a high ground spin state with uniaxial anisotropy, which leads to magnetic bistability from the individual molecule.[3] The specific linking of SMMs has been shown by the pioneering work of Wernsdorfer and co-workers on supramolecular dimers and 3D networks of tetranuclear manganese clusters.[4] Such a step-by-step assembly of SMMs or high-spin polynuclear complexes has produced a series of controlled coordination or supramolecular architectures.[5−7] Some of them exhibit interesting magnetic properties such as single-chain magnets, classical molecular-based magnets, or systems possessing an interplay between modified quantum and bulk thermodynamic properties.

In order to design such systems, it is crucial to prepare and select the polynuclear building block by considering its

*To whom correspondence should be addressed. Fax: +86-25-83314502. E-mail: zuojl@nju.edu.cn.

(1) (a) Sessoli, R.; Tsai, H.-L.; Schake, A. R.; Wang, S.; Vincent, J. B.; Folting, K.; Gatteschi, D.; Christou, G.; Hendrickson, D. N. *J. Am. Chem. Soc*. **1993**, *115*, 1804. (b) Sessoli, R.; Gatteschi, D.; Caneschi, A.; Novak, M. A. *Nature* **1993**, *365*, 141. (c) *Single-Molecule Magnets and Related Phenomena*; Winpenny, R. Ed.; Springer, Berlin, 2006; Structure and Bonding, Vol. *122*. (d) Gómez-Segura, J.; Veciana, J.; Ruiz-Molina, D. *Chem. Commun*. **2007**, 3699.

(2) (a) Krusin-Elbaum, L.; Shibauchi, T.; Argyle, B.; Gignac, L.; Weller, D. *Nature* **2001**, *410*, 444. (b) Chudnovsky E. M.; Tejada, J. *Macroscopic Quantum Tunneling of the Magnetic Moment*; Cambridge University Press, Cambridge, U.K., 1998. (c) Leuenberger, M. N.; Loss, D. *Nature* **2001**, *410*, 789. (d) Bogani, W.; Wernsdorfer *Nat. Mater*. **2008**, *7*, 179.

(3) (a) Gatteschi, D.; Sessoli, R. *Angew. Chem., Int. Ed*. **2003**, *42*, 268. (b) Christou, G.; Gatteschi, D.; Hendrickson, D. N.; Sessoli, R. *Mater. Res. Bull*. **2000**, *25*, 66.

(4) (a) Wernsdorfer, W.; Aliaga-Alcalde, N.; Hendrickson, D. N.; Christou, G. *Nature* **2002**, *416*, 406–409. (b) Tiron, R.; Wernsdorfer, W.; Aliaga-Alcalde, N.; Christou, G. *Phys. Rev. B* **2003**, *68*, 140407. (c) Wernsdorfer, W.; Bhaduri, S.; Vinslava, A.; Christou, G. *Phys. Rev. B* **2005**, *72*, 214429.

(5) (a) Miyasaka, H.; Nakata, K.; Sugiura, K.; Yamashita, M.; Clérac, R. *Angew. Chem., Int. Ed*. **2004**, *43*, 707. (b) Miyasaka, H.; Nakata, K.; Lecren, L.; Coulon, C.; Nakazawa, Y.; Fujisaki, T.; Sugiura, K.; Yamashita, M.; Clérac, R. *J. Am. Chem. Soc*. **2006**, *128*, 3770. (c) Lecren, L.; Roubeau, O.; Coulon, C.; Li, Y.-G.; Le Goff, X. F.; Wernsdorfer, W.; Miyasaka, H.; Clérac, R. *J. Am. Chem. Soc*. **2005**, *127*, 17353. (d) Yoo, J.; Wernsdorfer, W.; Yang, E.-C.; Nakano, M.; Rheingold, A. L.; Hendrickson, D. N. *Inorg. Chem*. **2005**, *44*, 3377. (e) Roubeau, O.; Clérac, R. *Eur. J. Inorg. Chem*. **2008**, 4325.

(6) (a) Boskovic, C.; Bircher, R.; Tregenna-Piggott, P. L. W.; Güdel, H. U.; Paulsen, C.; Wernsdorfer, W.; Barra, A.-L.; Khatsko, E.; Neels, A.; Stoeckli-Evans, H. *J. Am. Chem. Soc*. **2003**, *125*, 14046. (b) Yang, E.-C.; Wernsdorfer, W.; Zakharov, L. N.; Karaki, Y.; Yamaguchi, A.; Isidro, R. M.; Lu, G.-D.; Wilson, S. A.; Rheingold, A. L.; Ishimoto, H.; Hendrickson, D. N. *Inorg. Chem*. **2006**, *45*, 529. (c) Moushi, E. E.; Stamatatos, T. C.; Wernsdorfer, W.; Nastopoulos, V.; Christou, G.; Tasiopoulos, A. J. *Angew. Chem., Int. Ed*. **2006**, *45*, 7722. (d) Liu, C.-M.; Zhang, D.-Q.; Zhu, D.-B. *Chem. Commun*. **2008**, 368. (e) Stamatatos, T. C.; Abboud, K. A.; Wernsdorfer, W.; Christou, G. *Angew. Chem., Int. Ed*. **2008**, *47*, 6694.

(7) (a) Ferbinteanu, M.; Miyasaka, H.; Wernsdorfer, W.; Nakata, K.; Sugiura, K.; Yamashita, M.; Coulon, C.; Clérac, R. *J. Am. Chem. Soc*. **2005**, *127*, 3090. (b) Bai, Y.-L.; Tao, J.; Wernsdorfer, W.; Sato, O.; Huang, R.-B.; Zheng, L.-S. *J. Am. Chem. Soc*. **2006**, *128*, 16428. (c) Lecren, L.; Wernsdorfer, W.; Li, Y.-G.; Vindigni, A.; Miyasaka, H.; Clérac, R. *J. Am. Chem. Soc*. **2007**, *129*, 5045. (d) Xu, H.-B.; Wang, B.-W.; Pan, F.; Wang, Z.-M.; Gao, S. *Angew. Chem., Int. Ed*. **2007**, *46*, 7388. (e) Brockman, J. T.; Stamatatos, T. C.; Wernsdorfer, W.; Abboud, K. A.; Christou, G. *Inorg. Chem*. **2007**, *46*, 9160. (f) Chakov, N. E.; Wernsdorfer, W.; Abboud, K. A.; Christou, G. *Inorg. Chem*. **2004**, *43*, 5919.

Published on Web 04/29/2009

structure, magnetic properties, and affinity to be connected in networks. In our previous work, we employed the tris(pyrazolyl)borate tricyanometalate precursor to generate a series of interesting cyano-bridged clusters exhibiting SMM-type behavior.[8] Recently, tris(indazolyl)hydroborate (Tp^{4Bo}) has been used instead of tris(pyrazolyl)hydroborate (Tp) in the tricyanometallate system to construct multinuclear clusters and analyze the influence of this substitution on the magnetic properties (Chart 1).[9] As we know, the introduction of the indazolyl moieties is possible to increase noncovalent or weak interactions involving aromatic rings such as face-to-face $\pi-\pi$ stacking interactions and point-to-face C−H$\cdots\pi$ interactions.[10] In this paper, we report the syntheses of six cyano-bridged clusters based on a Tp^{4Bo} tricyanometalate precursor, $[(Tp^{4Bo})_6Fe_6(CN)_{18}M_2Na_2(H_2O)_{16}]\cdot 4H_2O$ (M = Cu, Co, Mn; **1**−**3**) and $[(Tp^{4Bo})_6Fe_6(CN)_{18}M_2Na_2(H_2O)_{12}(DMF)_4]\cdot H_2O$ (M = Cu, Co, Mn; **4**−**6**). The detailed studies of their crystal structures and magnetic properties are also described.

Experimental Section

Synthesis. All chemicals were reagent-grade and were used as received. $(Bu_4N)[(Tp^{4Bo})Fe(CN)_3]\cdot H_2O\cdot 2MeCN$ was prepared according to literature methods.[9]

Caution! *The cyanides are very toxic, and perchlorate salts are potentially explosive. Thus, these starting materials should be handled in small quantities and with great caution.*

Preparation of Complex $Na[(Tp^{4Bo})Fe(CN)_3]$. Solid $NaClO_4$ (122.4 mg, 1 mmol) was added to a solution of $(Bu_4N)[(Tp^{4Bo})Fe(CN)_3]\cdot H_2O\cdot 2MeCN$ (840.0 mg, 1 mmol) in 10 mL of acetonitrile, resulting in immediate formation of a red−brown precipitate. The red−brown product was collected by filtration and washed with acetonitrile and ether. Yield: 92%. Anal. calcd (%) for $C_{24}H_{16}BFeNaN_9$: C, 55.42; H, 3.10; N, 24.24. Found: C, 55.27; H, 3.45; N, 24.06. IR (KBr, cm^{-1}): 2119 (ν_{CN}).

Preparation of Complex $[(Tp^{4Bo})_6Fe_6(CN)_{18}Cu_2Na_2(H_2O)_{16}]\cdot 4H_2O$ (1). A mixture of CH_3OH and H_2O (v/v, 2:1, 3 mL) was gently layered on the top of a 2 mL water solution of $Na[(Tp^{4Bo})Fe(CN)_3]$ (52.0 mg, 0.1 mmol). A solution of $Cu(ClO_4)_2\cdot 6H_2O$ (37.0 mg, 0.1 mmol) in 2 mL of CH_3OH was added carefully as a third layer. Black block crystals of **1** were obtained after two weeks; they were washed with ethanol and ether and dried in the air. Yield: 35%. Anal. calcd (%) for $C_{144}H_{136}B_6Cu_2Fe_6N_{54}Na_2O_{20}$: C, 49.19; H, 3.90; N, 21.51. Found: C, 49.01; H, 3.98; N, 21.37%. IR (KBr, cm^{-1}): 2126, 2167 (ν_{CN}).

Preparation of Complex $[(Tp^{4Bo})_6Fe_6(CN)_{18}Co_2Na_2(H_2O)_{16}]\cdot 4H_2O$ (2). This was prepared by a similar procedure to that described for **1** except that $Co(ClO_4)_2\cdot 6H_2O$ was used. Yield: 39%. Anal. calcd (%) for $C_{144}H_{136}B_6Co_2Fe_6N_{54}Na_2O_{20}$: C, 49.32; H, 3.91; N, 21.57. Found: C, 49.09; H, 4.02; N, 21.41%. IR (KBr, cm^{-1}): 2126, 2156 (ν_{CN}).

Chart 1

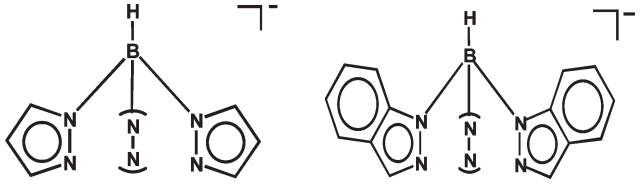

Tp Tp^{4Bo}

Preparation of Complex $[(Tp^{4Bo})_6Fe_6(CN)_{18}Mn_2Na_2(H_2O)_{16}]\cdot 4H_2O$ (3). This was prepared by a similar procedure to that described for **1** except that $Mn(ClO_4)_2\cdot 6H_2O$ was used. Yield: 43%. Anal. calcd (%) for $C_{144}H_{136}B_6Mn_2Fe_6N_{54}Na_2O_{20}$: C, 49.43; H, 3.92; N, 21.62. Found: C, 49.16; H, 4.05; N, 21.47%. IR (KBr, cm^{-1}): 2126, 2150 (ν_{CN}).

Preparation of Complex $[(Tp^{4Bo})_6Fe_6(CN)_{18}Cu_2Na_2(H_2O)_{12}(DMF)_4]\cdot H_2O$ (4). A mixture of DMF and H_2O (v/v, 2:1, 3 mL) was gently layered on the top of a 2 mL water solution of $Na[(Tp^{4Bo})Fe(CN)_3]$ (52.0 mg, 0.1 mmol). A solution of $Cu(ClO_4)_2\cdot 6H_2O$ (37.0 mg, 0.1 mmol) in 2 mL of DMF was added carefully as a third layer. Black block crystals of **4** were obtained after one week; they were washed with ethanol and ether and dried in the air. Yield: 38%. Anal. calcd (%) for $C_{156}H_{150}B_6Cu_2Fe_6N_{58}Na_2O_{17}$: C, 50.88; H, 4.11; N, 22.06. Found: C, 50.68; H, 4.17; N, 21.90%. IR (KBr, cm^{-1}): 2128, 2169 (ν_{CN}).

Preparation of Complex $[(Tp^{4Bo})_6Fe_6(CN)_{18}Co_2Na_2(H_2O)_{12}(DMF)_4]\cdot H_2O$ (5). This was prepared by a similar procedure to that described for **4** except that $Co(ClO_4)_2\cdot 6H_2O$ was used. Yield: 41%. Anal. calcd (%) for $C_{156}H_{150}B_6Co_2Fe_6N_{58}Na_2O_{17}$: C, 51.01; H, 4.12; N, 22.12. Found: C, 49.87; H, 4.24; N, 22.06%. IR (KBr, cm^{-1}): 2129, 2161 (ν_{CN}).

Preparation of Complex $[(Tp^{4Bo})_6Fe_6(CN)_{18}Mn_2Na_2(H_2O)_{12}(DMF)_4]\cdot H_2O$ (6). This was prepared by a similar procedure to that described for **4** except that $Mn(ClO_4)_2\cdot 6H_2O$ was used. Yield: 48%. Anal. calcd (%) for $C_{156}H_{150}B_6Mn_2Fe_6N_{58}Na_2O_{17}$: C, 51.12; H, 4.13; N, 22.17. Found: C, 51.04; H, 4.19; N, 22.04%. IR (KBr, cm^{-1}): 2127, 2152 (ν_{CN}).

X-Ray Structure Determination. The crystal structures were determined on a Siemens (Bruker) SMART CCD diffractometer using monochromated Mo Kα radiation (λ = 0.71073 Å) at 291 K. Cell parameters were retrieved using SMART software and refined using SAINT[11] on all observed reflections. Data were collected using a narrow-frame method with scan widths of 0.30° in ω and an exposure time of 10 s/frame. The highly redundant data sets were reduced using SAINT[11] and corrected for Lorentz and polarization effects. Absorption corrections were applied using SADABS,[12] supplied by Bruker. Structures were solved by direct methods using the program SHELXL-97.[13] The positions of metal atoms and their first coordination spheres were located from direct-methods *E*-maps; other non-hydrogen atoms were found in alternating difference Fourier syntheses and least-squares refinement cycles and, during the final cycles, refined anisotropically. Hydrogen atoms were placed in calculated position and refined as riding atoms with a uniform value of U_{iso}. Final crystallographic data and values of R_1 and wR_2 are listed in Table 1. Relevant bond distances and angles are listed in Tables S1−S6 (Supporting Information), respectively.

(8) (a) Wang, S.; Zuo, J. L.; Zhou, H. C.; Choi, H. J.; Ke, Y. X.; Long, J. R.; You, X. Z. *Angew. Chem., Int. Ed.* **2004**, *43*, 5940. (b) Wang, C. F.; Zuo, J. L.; Bartlett, B. M.; Song, Y.; Long, J. R.; You, X. Z. *J. Am. Chem. Soc.* **2006**, *128*, 7162. (c) Liu, W.; Wang, C. F.; Li, Y. Z.; Zuo, J. L.; You, X. Z. *Inorg. Chem.* **2006**, *45*, 10058. (d) Wang, C. F.; Liu, W.; Song, Y.; Zhou, X. H.; Zuo, J. L.; You, X. Z. *Eur. J. Inorg. Chem.* **2008**, 717. (e) Gu, Z. G.; Yang, Q. F.; Liu, W.; Song, Y.; Li, Y. Z.; Zuo, J. L.; You, X. Z. *Inorg. Chem.* **2006**, *45*, 8895.

(9) Gu, Z. G.; Liu, W.; Yang, Q. F.; Zhou, X. H.; Zuo, J. L.; You, X. Z. *Inorg. Chem.* **2007**, *46*, 3236.

(10) (a) Janiak, C.; Temizdemir, S.; Dechert, S.; Deck, W.; Girgsdies, F.; Heinze, J.; Kolm, M. J.; Scharmann, T. G.; Zipffel, O. M. *Eur. J. Inorg. Chem.* **2000**, 1229. (b) Craven, E.; Mutlu, E.; Lundberg, D.; Temizdemir, S.; Dechert, S.; Brombacher, H.; Janiak, C. *Polyhedron* **2002**, *21*, 553.

(11) *SAINT-Plus*, version 6.02; Bruker Analytical X-ray System: Madison, WI, 1999.

(12) Sheldrick, G. M. *SADABS*; Bruker Analytical X-ray Systems: Madison, WI, 1996.

(13) Sheldrick, G. M. *SHELXTL-97*; Universität of Göttingen: Göttingen, Germany, 1997.

Table 1. Summary of Crystallographic Data for the Complexes **1**−**6**

	1	**2**	**3**	**4**	**5**	**6**
formula	$C_{144}H_{136}B_6Cu_2Fe_6N_{54}Na_2O_{20}$	$C_{144}H_{136}B_6Co_2Fe_6N_{54}Na_2O_{20}$	$C_{144}H_{136}B_6Fe_6Mn_2N_{54}Na_2O_{20}$	$C_{156}H_{150}B_6Cu_2Fe_6N_{58}Na_2O_{17}$	$C_{156}H_{150}B_6Co_2Fe_6N_{58}Na_2O_{17}$	$C_{156}H_{150}B_6Fe_6Mn_2N_{58}Na_2O_{17}$
fw	3516.09	3506.87	3498.89	3682.36	3673.14	3665.16
cryst syst	monoclinic	monoclinic	monoclinic	monoclinic	monoclinic	monoclinic
space group	$P2_1/c$	$P2_1/c$	$P2_1/c$	$P2_1/n$	$P2_1/n$	$P2_1/n$
a, Å	14.079(6)	13.960(8)	13.960(3)	14.093(2)	13.932(8)	13.988(4)
b, Å	26.050(3)	27.014(3)	27.108(4)	26.871(5)	26.414(3)	26.577(6)
c, Å	27.039(5)	27.227(3)	27.355(3)	23.298(4)	23.704(3)	23.826(6)
β, deg	120.670(4)	120.447(5)	120.541(8)	90.354(4)	91.597(2)	91.659(5)
V, Å^3	8530.1(1)	8852.3(1)	8916(3)	8823(3)	8720.2(1)	8854(4)
Z	2	2	2	2	2	2
D_{calcd}, g cm^{-3}	1.369	1.316	1.303	1.386	1.399	1.375
T/K	291(2)	291(2)	291(2)	291(2)	291(2)	291(2)
μ, mm^{-1}	0.821	0.738	0.689	0.797	0.752	0.696
θ, deg	1.68−26.00	1.64−26.00	1.15−26.00	1.75−26.00	1.65−26.00	1.75−26.00
F(000)	3608	3600	3592	3788	3780	3772
index ranges	$-16 \le h \le 17$, $-32 \le k \le 31$, $-32 \le l \le 33$	$-10 \le h \le 17$, $-33 \le k \le 30$, $-33 \le l \le 25$	$-17 \le h \le 16$, $-33 \le k \le 33$, $-30 \le l \le 30$	$-17 \le h \le 16$, $-32 \le k \le 33$, $-28 \le l \le 25$	$-17 \le h \le 17$, $-19 \le k \le 32$, $-29 \le l \le 28$	$-17 \le h \le 15$, $-32 \le k \le 32$, $-29 \le l \le 24$
data/restraints/params	16725/0/1153	17363/0/1153	17222/0/1153	17260/0/1171	17139/6/1171	17359/0/1184
GOF (F^2)	1.078	1.092	1.081	1.098	1.077	0.998
R_1,[a] wR_2[b] ($I > 2\sigma(I)$)	0.0626, 0.1462	0.0652, 0.1246	0.0599, 0.1283	0.0501, 0.0735	0.0532, 0.0854	0.0482, 0.0957
R_1,[a] wR_2[b] (all data)	0.1027, 0.1583	0.1025, 0.1340	0.0816, 0.1357	0.0811, 0.0781	0.0850, 0.0908	0.0781, 0.1015

[a] $R_1 = \sum||F_o| - |F_c||/\sum|F_o|$. [b] $wR_2 = [\sum w(F_o^2 - F_c^2)^2/\sum w(F_o^2)]^{1/2}$.

Physical Measurements. Elemental analyses for C, H, and N were performed on a Perkin-Elmer 240C analyzer. Infrared spectra were recorded on a Vector22 Bruker Spectrophotometer with KBr pellets in the 400−4000 cm^{-1} region. Magnetic measurements were performed on polycrystalline samples with a Quantum Design MPMS-XL7 SQUID magnetometer. Direct current magnetic susceptibility was measured over the temperature range 1.8−300 K with an applied magnetic field of 2 kOe. Field dependences of magnetization were measured using a flux magnetometer in the applied field up to 70 kOe generated by a conventional pulsed technique. Data were corrected for the diamagnetic contribution calculated from Pascal constants. Alternating current measurements were performed at various frequencies from 1 to 1500 Hz with an ac field amplitude of 5 Oe and no dc field applied. Samples (ca. 15 mg) were restrained with petroleum jelly to prevent torquing of the crystallites.

Results and Discussions

Structural Description. Complexes **1**−**3** and **4**−**6** are isostructural, respectively. Complexes **1**−**3** crystallize in the same monoclinic space group, $P2_1/c$, while **4**−**6** crystallize in $P2_1/n$. All six complexes have similar core structures, and they are centrosymmetric and contain two symmetry-related $[(Tp^{4Bo})_3Fe_3(CN)_9M(Sov)_2(H_2O)]^-$ (M = Cu, Co, Mn; Sov = H_2O for **1**−**3**; Sov = DMF for **4**−**6**) subunits, related to each other by an inversion center ($-x + 1, -y + 2, -z + 2$ for **1**−**3**; $-x + 1, -y + 1, -z + 1$ for **4**−**6**), situated between the two sodium atoms (Figure 1). The main difference between **1**−**3** and **4**−**6** is that, in complexes **1**−**3**, there are three water molecules coordinated to each copper (or cobalt, manganese) atom; in complexes **4**−**6**, each metal atom is surrounded by one water and two DMF molecules. Selected mean interatomic distances and angles from all six crystal structures are provided in Table 2 for comparison. As a representative example, Figure 1 depicts the structure of the $[(Tp^{4Bo})_6Fe_6(CN)_{18}Cu_2Na_2(H_2O)_{16}]$ cluster in **1**. Inside each subunit of **1**, a central $[Cu(H_2O)_3]^{2+}$ core is linked to three $[(Tp^{4Bo})Fe(CN)_3]^-$ ions via bridging cyanides in the meridional arrangement forming a $Fe_3^{III}Cu^{II}$ T-shaped geometry. The cyanide bridges deviate from linearity, with different C≡N−Cu angles (C(2)−N(7)−Cu(1), 169.1(3)°; C(7)−N(25)−Cu(1), 160.7(3)°; C(4)−N(11)−Cu(1), 149.7(3)°), which are also found in other T-shaped cyanide-bridge clusters.[14] The central copper atom has a distorted octahedron coordination constructed by three oxygen atoms from coordinated water molecules and three cyanide nitrogen atoms (Cu−N, 2.098(4)−2.137(3) Å; Cu−O, 2.18(3)−2.21(3) Å). The Fe−C (1.845(4)−1.947(4) Å) and Fe−N (1.904(3)−1.998(3) Å) bond lengths are in good agreement with those reported previously for structures containing low-spin tricyano iron(III) complexes,[15,16] and the Fe−C≡N (174.3(3)°−178.8(3)°) angles are a little deviated from linearity. The two subunits are bridged by the two sodium cations, through two cyano bridges and two coordinated water molecules. The coordination around the sodium atoms is distorted pentagonal bipyramidal, with N8, O4,

(14) (a) Herchel, R.; Boča, R.; Gembický, M.; Kožíš, J.; Renz, F. *Inorg. Chem.* **2004**, *43*, 4103. (b) Miyasaka, H.; Takahashi, H.; Madanbashi, T.; Sugiura, K.; Clérac, R.; Nojiri, H. *Inorg. Chem.* **2005**, *44*, 5969.

(15) (a) Lescouëzec, R.; Vaissermann, J.; Lloret, F.; Julve, M.; Verdaguer, M. *Inorg. Chem.* **2002**, *41*, 5943. (b) Kim, J.; Han, S.; Pokhodnya, K. I.; Migliori, J. M.; Miller, J. S. *Inorg. Chem.* **2005**, *44*, 6983. (c) Yang, J. Y.; Shores, M. P.; Sokol, J. J.; Long, J. R. *Inorg. Chem.* **2003**, *42*, 1403. (d) Lescouëzec, R.; Vaissermann, J.; Toma, L. M.; Carrasco, R.; Lloret, F.; Julve, M. *Inorg. Chem.* **2004**, *43*, 2234. (e) Ni, Z.-H.; Kou, H.-Z.; Zhang, L.-F.; Ni, W.-W.; Jiang, Y.-B.; Cui, A.-L.; Ribas, J.; Sato, O. *Inorg. Chem.* **2005**, *44*, 9631.

(16) (a) Li, D.; Parkin, S.; Wang, G.; Yee, G. T.; Prosvirin, A. V.; Holmes, S. M. *Inorg. Chem.* **2005**, *44*, 4903. (b) Li, D.; Parkin, S.; Wang, G.; Yee, G. T.; Holmes, S. M. *Inorg. Chem.* **2006**, *45*, 1951. (c) Li, D.; Clérac, R.; Parkin, S.; Wang, G.; Yee, G. T.; Holmes, S. M. *Inorg. Chem.* **2006**, *45*, 5251. (d) Li, D.; Parkin, S.; Wang, G.; Yee, G. T.; Clérac, R.; Wernsdorfer, W.; Holmes, S. M. *J. Am. Chem. Soc.* **2006**, *128*, 4214. (e) Li, D.; Parkin, S.; Clérac, R.; Holmes, S. M. *Inorg. Chem.* **2006**, *45*, 7569.

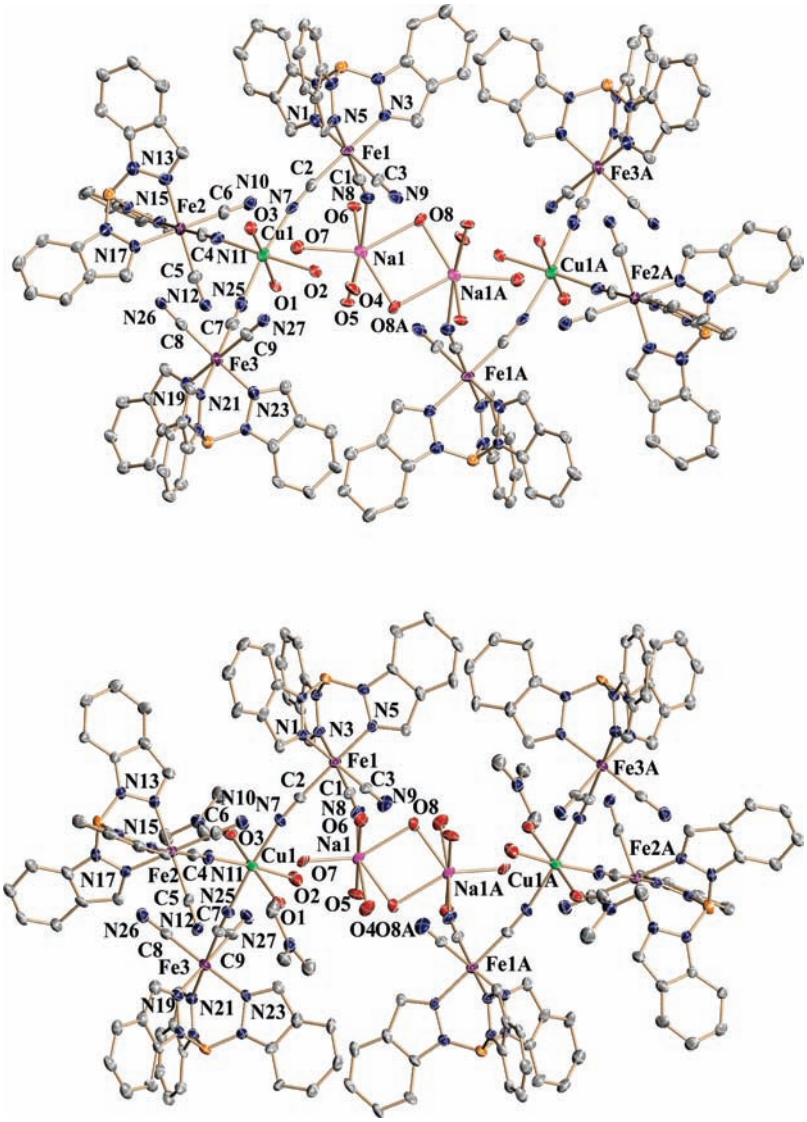

Figure 1. Perspective drawing of complexes **1** (up) and **4** (bottom) showing the atom numbering. Thermal ellipsoids are drawn at the 30% probability levels. Hydrogen atoms are omitted for clarity.

O7, O8, and O8A equatorial and O5 and O6 axial donor atoms (Na−N/O_{basal}, 2.32(4)−2.55(6) Å; Na−O_{apical}, 2.23(3)−2.33(6) Å). $[(Tp^{4Bo})_3Fe_3(CN)_9Cu(H_2O)_3]^-$ subunit presents an almost planar central core, defined by atoms Fe1, Fe2, Fe3, and Cu1, which parallels the symmetry-related mean plane. The two parallel planes form angle of 68.21° with the plane defined by atoms Na1, O8, O8A, and Na1A (Figure S1, Supporting Information). The shortest intramolecular $Fe^{III}\cdots Cu^{II}$, $Fe^{III}\cdots Fe^{III}$, and $Cu^{II}\cdots Cu^{II}$ separations for **1** are 5.000, 7.373, and 15.491 Å, respectively. Whereas, the shortest intermolecular $Fe^{III}\cdots Cu^{II}$, $Fe^{III}\cdots Fe^{III}$, and $Cu^{II}\cdots Cu^{II}$ distances for **1** are 7.554, 6.969, and 8.776 Å, respectively.

Very interestingly, each polynuclear cluster in **1** strongly interacts with 12 adjacent such units through face-to-face $\pi-\pi$ stacking interactions with a centroid-to-centroid distance in the range of about 3.498−3.663 Å, leading to a 3D microporous supramolecular framework (Figure 2). The 3D framework can be rationalized as a 12-connected net by assigning the polynuclear cluster $[(Tp^{4Bo})_6Fe_6(CN)_{18}Cu_2Na_2(H_2O)_{16}]$ as a node and the $\pi-\pi$ stacking interaction as a linker (Figure 3b). The distances from the center of the central cluster unit to adjacent unit centers are 18.773, 23.259, 27.039, and 27.292 Å, and each unit resides at a crystallographic inversion center. The majority of reported 12-connected frameworks thus far adopt close-packed structures, either hexagonal close-packed or face-centered cubic close-packed.[17] Surprisingly, the linking of the 12 nodes in **1** are hexagonal open-packed with no connections between the six apical nodes and the six basal nodes. In the *bc* plane, each center links six adjacent centers, forming a 3^6 net. The high-connected and complex structures in **1** can be described as being formed from parallel 2D 3^6 subnet tectons, with each center providing six linkers to centers in adjacent nets, three on each side (Figure 3a). To the best of our knowledge, complex **1** is a new 12-connected topological network and represents the

(17) (a) Hill, R. J.; Long, D. L.; Champness, N. R.; Hubberstey, P.; Schröder, M. *Acc. Chem. Res.* **2005**, *38*, 335. (b) Zhang, X. M.; Fang, R. Q.; Wu, H. S. *J. Am. Chem. Soc.* **2005**, *127*, 7670. (c) Li, D.; Wu, T.; Zhou, X. P.; Zhou, R.; Huang, X. C. *Angew. Chem., Int. Ed.* **2005**, *44*, 4175.

Table 2. Selected Mean Interatomic Distances and Angles for **1**−**6**

	1	2	3	4	5	6
Fe−C	1.890(4)	1.915(4)	1.919(4)	1.905(3)	1.896(3)	1.908(3)
Fe−N	1.949(5)	1.973(3)	1.975(3)	1.978(2)	1.970(2)	1.979(4)
M−N	2.118(4)	2.155(3)	2.169(3)	2.139(2)	2.132(2)	2.142(2)
M−O	2.191(3)	2.186(3)	2.207(3)	2.185(2)	2.191(2)	2.192(3)
Na−N	2.408(4)	2.454(3)	2.460(3)	2.258(3)	2.231(3)	2.246(3)
Na−O	2.37(3)	2.41(3)	2.43(3)	2.22(2)	2.21(3)	2.20(2)
Fe···M	5.016(3)	5.090(2)	5.105(2)	5.124(7)	5.000(7)	5.130(1)
Fe···Fe	8.466(9)	8.590(1)	8.615(6)	8.627(2)	8.594(3)	8.641(8)
M···M	15.491(2)	15.480(3)	15.529(5)	15.678(7)	15.484(6)	15.540(2)
Na···Na	3.738(5)	3.780(7)	3.793(2)	3.443(5)	3.494(5)	3.505(5)
Fe−C−N	177.3(6)	177.1(3)	177.4(3)	177.5(3)	177.3(3)	177.1(4)
C−N−M	159.8(3)	160.3(2)	159.8(3)	162.6(2)	162.4(3)	162.6(2)
C−N−Na	152.7(3)	152.9(2)	152.9(2)	163.53(2)	163.65(2)	163.21(2)
C−Fe−C	88.2(3)	87.5(2)	87.25(2)	87.47(4)	87.61(2)	87.56(4)
C−Fe−N	91.05(3)	91.89(3)	92.01(3)	91.89(3)	91.73(3)	91.75(3)
N−Fe−N	89.67(3)	88.73(2)	88.73(2)	88.74(4)	88.92(3)	88.93(3)
N−M−N	120.00(3)	120.00(3)	120.00(3)	120.00(3)	120.00(3)	120.00(3)
N−M−O	97.8(2)	97.6(3)	97.8(3)	99.9(2)	100.1(2)	99.9(1)
O−M−O	118.3(3)	119.0(2)	119.1(2)	111.3(6)	111.2(6)	111.1(4)
N−Na−O	110.6(3)	113.8(4)	113.2(4)	112.6(1)	112.8(8)	112.4(2)
O−Na−O	98.2(1)	97.0(3)	97.6(6)	98.6(2)	98.5(3)	98.6(3)
Na−O−Na	98.3(2)	94.9(8)	96.8(1)	94.7(6)	96.4(1)	96.2(2)

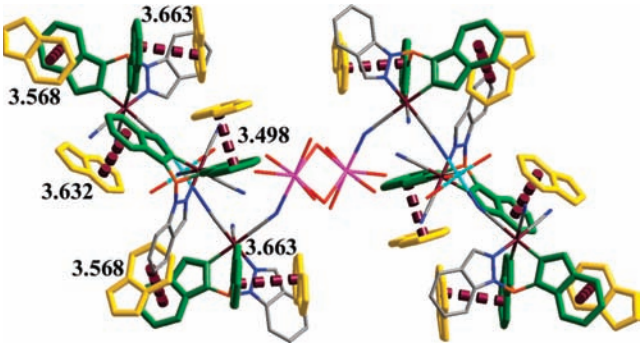

Figure 2. Perspective drawing of complex **1** showing the $\pi-\pi$ stacking interactions. Green indazolyl moieties belong to the central cluster, while yellow indazolyl moieties belong to 12 adjacent clusters.

highest connected topology of any supramolecular architectures with $\pi-\pi$ stacking interactions.

Magnetic Properties. Magnetic measurements were performed on polycrystalline samples of complexes **1**−**6**. The magnetic property of the tricyanometallate building block, $(Bu_4N)[(Tp^{4Bo})Fe(CN)_3]\cdot H_2O\cdot 2MeCN$, has been reported in our previous paper.[9] The $\chi_M T$ value monotonically decreases from 0.66 emu K mol^{-1} to 0.33 emu K mol^{-1} as the temperature is lowered from 300 to 1.8 K (Figure S2, Supporting Information). The $\chi_M T$ value at room temperature is significantly larger than the spin-only value expected for an isolated low-spin octahedral iron(III) ion (0.375 emu K mol^{-1}, $S = 1/2$, $g = 2.0$), which is similar to those reported for other low-spin cyano-containing mononuclear iron(III) species.[18,8d,16b] It indicates that there exists a significant spin−orbit coupling of the $^2T_{2g}$ ground term for iron(III) ions.[19] A g_{Fe} value of ca. 2.65 can be calculated from the $\chi_M T$ data of $(Bu_4N)[(Tp^{4Bo})Fe(CN)_3]$. The examination of the ground state is carried out by field-dependent magnetization measurements at 1.8 K. The data are in excellent

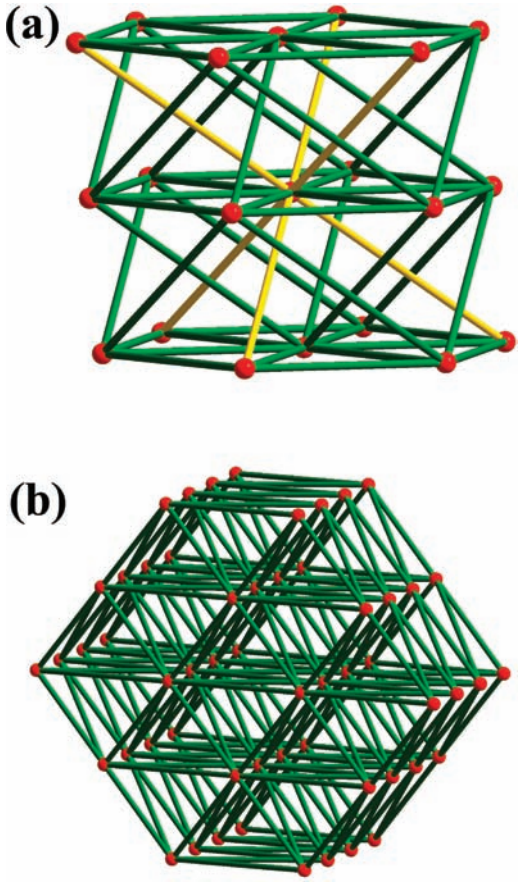

Figure 3. Perspective drawing of 3D supramolecular architecture through the $\pi-\pi$ stacking interactions of **1**. Red ball: $[(Tp^{4Bo})_6Fe_6(CN)_{18}M_2Na_2(H_2O)_{12}(sov)_4]$ (M = Cu, Co, Mn; sov = H_2O, DMF). (a) The linking of the 3^6 net. (b) The 3D 12-connected framework.

(18) (a) Patra, A. K.; Ray, M.; Mukherjee, R. *Inorg. Chem.* **2000**, *39*, 652. (b) Lescouëzec, R.; Lloret, F.; Julve, M.; Vaissermann, J.; Verdaguer, M.; Llusar, R.; Uriel, S. *Inorg. Chem.* **2001**, *40*, 2065. (c) Toma, L. M.; Lescouëzec, R.; Pasán, J.; Ruiz-Pérez, C.; Vaissermann, J.; Cano, J.; Carrasco, R.; Wernsdorfer, W.; Lloret, F.; Julve, M. *J. Am. Chem. Soc.* **2006**, *128*, 4842.

(19) (a) Martin, L. L.; Martin, R. L.; Murray, K. S.; Sargeson, A. M. *Inorg. Chem.* **1990**, *29*, 1387. (b) Carlin, R. L. *Magnetochemistry*; Springer-Verlag: New York, 1986. (c) Kahn, O. *Molecular Magnetism*; Verlag Chemie: Weinheim, Germany, 1993.

agreement with the Brillouin function for one noninteracting $S = 1/2$ ion (Figure S3, Supporting Information).

The susceptibility variation at different temperatures of **1** and **4** were measured at 1.8−300 K (Figure 4). At room temperature, the $\chi_M T$ values are 2.19 and 2.13 emu K mol^{-1} for **1** and **4**, respectively, which are lower than the spin-only value of 2.35 emu K mol^{-1} for three low-spin Fe^{III} ($S = 1/2$ and $g = 2.65$) and one Cu^{II} ($S = 1/2$ and assuming $g = 2$) ion. This behavior has also been observed in other $[(Tp)Fe^{III}(CN)_3]^-$−Cu^{II} complexes,[8a,8c,9] but the reasons have not been clarified so far. With decreasing temperature, $\chi_M T$ increase, reaching the maximum values of 2.77 and 3.13 emu K mol^{-1} at approximately 7 K for **1** and **4**, respectively, suggesting that ferromagnetic coupling resulted from the orthogonal spin orbitals of the Fe^{III} (t_{2g}) and square-pyramidal Cu^{II} (b_{1g}) centers. The maximum values are consistent with a ground state spin of $S = 2$ for the $Fe_3^{III}Cu^{II}$ clusters. This magnetic nature could be further supported by the apparently unsaturated magnetization values of 3.71 and 3.79 Nβ mol^{-1} under a 7 T magnetic field at 1.8 K for **1** and **4**, respectively, confirming the $S = 2$ ground state for the two clusters (inset in Figure 4). The low-field magnetization values are fitted well with the Brillouin curve corresponding to $S = 2$ and are higher than the Brillouin curve for noninteracting $S = 3 \times S_{Fe} + S_{Cu}$ with $g = 2.0$, confirming the overall ferromagnetic Cu^{II}−Fe^{III} interaction. The high-field magnetizations are lower than calculated values, which may be due to the zero-field splitting effect. Below 7 K, $\chi_M T$ sharply drops to 1.82 and 2.02 emu K mol^{-1} at 1.8 K for **1** and **4**, respectively, which are attributed to the presence of zero-field splitting and intermolecular interactions. According to the structures, the exchange Hamiltonian of **1** and **4** can be described as $\hat{H} = -2J\hat{S}_{Cu1}(\hat{S}_{Fe1} + \hat{S}_{Fe2} + \hat{S}_{Fe3})$.

$$\chi_M = \frac{2Ng^2\beta^2}{kT} \times \frac{1 + 5e^{4J/kT} + 2e^{3J/kT}}{3 + 5e^{4J/kT} + 2e^{J/kT} + 3e^{3J/kT}} \quad (1)$$

where J represents the average interactions between Cu^{II} and Fe^{III} ions; the magnetic susceptibilities above 7 K were simulated using eq 1 with a TIP correction, giving the best fit with parameters $g = 2.15$ and 2.11, $J_1 = 2.72$ and 5.39 cm^{-1}, TIP $= 1.5 \times 10^{-4}$ and 9.0×10^{-5} emu/mol, and $R = 1.5 \times 10^{-4}$ and 1.6×10^{-4} for **1** and **4**, respectively. The small positive J values indicate that the exchange coupling within **1** and **4** is ferromagnetic but rather weak. The J values for **1** and **4** are smaller than those observed for other cyanide-bridged cluster-containing low-spin iron(III) and copper(II) ions.[20,8b−8d] The slight variation of J in these complexes is mainly due to the structural differences, and the aforementioned face-to-face π−π interactions between neighboring clusters in **1** and **4** could mediate weak antiferromagnetic coupling, which potentially attenuates the ferromagnetic coupling. Such noncovalent pathways have been invoked previously in rationalizing the origin of magnetic coupling in numerous related situations.[21]

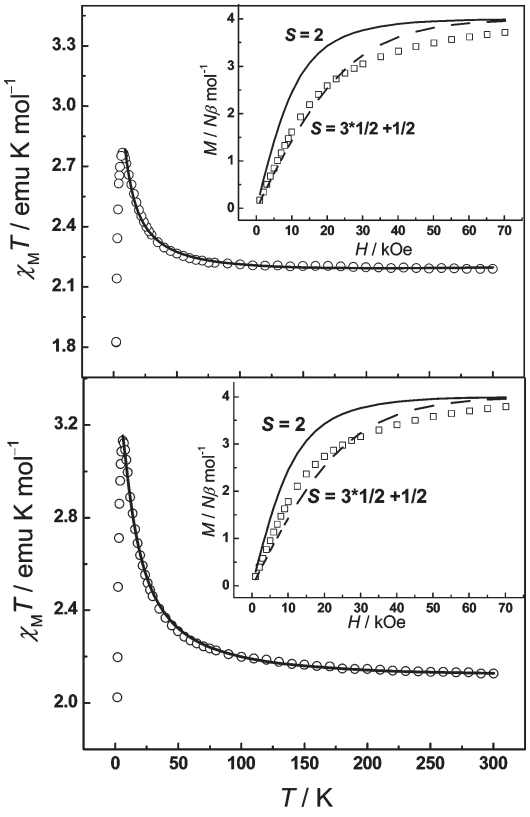

Figure 4. Plots of $\chi_M T$ versus T for **1** (up) and **4** (bottom) at a field of 2 KOe. Solid lines represent the best fitting of the data. The insets show magnetization versus field up to $H = 70$ kOe at 1.8 K for **1** (up) and **4** (bottom); the lines represent the Brillouin function that corresponds to noninteracting $S = 3 \times S_{Fe}^{III} + S_{Cu}^{II}$ (dotted) and $S = 2$ (solid) with $g = 2.0$.

The magnetization variations for **1** and **4** at different magnetic fields were recorded between 1.8 and 5 K (Figure 5). The nonsuperposition of the isofield lines indicates the presence of significant zero-field splitting. With the spin ground state $S = 2$, fits of the magnetization data using ANISOFT[22] for $T \leq 5$ K and $H \geq 1$ T afforded $D = -1.45$ and -1.55 cm^{-1} and $g = 1.95$ and 1.99 for **1** and **4**, respectively. The sign of the fitted D parameter may be not reliable, but the fitting results suggest appreciable magnetic anisotropies in **1** and **4**. The ac susceptibility studies carried out in the 1.8−10 K range in a 5 Oe oscillating field at frequencies up to 1500 Hz for **1** and **4** showed no evidence for magnetic ordering or slow paramagnetic relaxation.

The temperature dependence of susceptibility for **2** and **5** is displayed in Figure 6. The room-temperature $\chi_M T$ values are 5.14 and 5.27 emu K mol^{-1} for **2** and **5**, respectively. Assuming $g_{Fe} = 2.65$ for the building block, we conclude that the g_{Co} values are 2.60 and 2.65 for **2** and **5**, respectively, confirming the spin−orbit coupling effects of the Co^{II} and Fe^{III} centers. Upon lowering the temperature, the $\chi_M T$ values decrease continuously and

(20) (a) Oshio, H.; Tamada, O.; Onodera, H.; Ito, T.; Ikoma, T.; Tero-Kubota, S. *Inorg. Chem.* **1999**, *38*, 5686. (b) Oshio, H.; Yamamoto, M.; Ito, T. *Inorg. Chem.* **2002**, *41*, 5817.

(21) (a) Bagai, R.; Wernsdorfer, R.; Abboud, K. A.; Christou, G. *J. Am. Chem. Soc.* **2007**, *129*, 12918. (b) Desplanches, C.; Ruiz, E.; Rodríguez-Fortea, A.; Alvarez, S. *J. Am. Chem. Soc.* **2002**, *124*, 5197. (c) Yang, J. Y.; Shores, M. P.; Sokol, J. J.; Long, J. R. *Inorg. Chem.* **2003**, *42*, 1403. (d) Langenberg, K. V.; Batten, S. R.; Berry, K. J.; Hockless, D. C. R.; Moubaraki, B.; Murray, K. S. *Inorg. Chem.* **1997**, *36*, 5006.

(22) Shores, M. P.; Sokol, J. J.; Long, J. R. *J. Am. Chem. Soc.* **2002**, *124*, 2279.

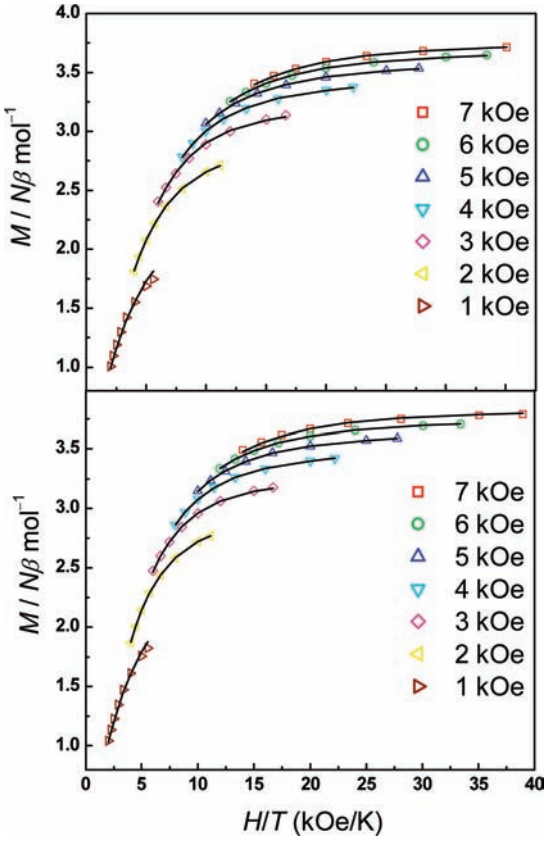

Figure 5. Plots of magnetization vs H/T for **1** (up) and **4** (bottom) between 1.8 and 5 K. Solid lines represent the best fits to the data.

reach 4.09 emu K mol^{-1} at 20 K for **2** and 4.07 emu K mol^{-1} at 26 K for **5**, followed by a slight increase with a maximum of 4.12 emu K mol^{-1} at 9 K for **2** and 4.26 emu K mol^{-1} at 8 K for **5**. The maxima correspond to an $S = 2$ ground state with $g = 2.34$ and 2.38. Then, $\chi_M T$ values drop to 2.45 and 2.82 emu K mol^{-1} at 1.8 K for **2** and **5**, respectively. The decrease of $\chi_M T$ values in the high-temperature regions may come from the orbital contribution from Co^{II} or the depopulation of low-lying excited states. The magnetization at saturation per $Fe_3^{III}Co^{II}$ unit is 4.92 and 4.89 Nβ mol^{-1} at 7 T for **2** and **5**, respectively, also suggesting $S = 2$ for **2** and **5** (insert of Figure 6), which can be confirmed by simulation of the Brillouin curves corresponding to both $S = 2$ and noninteracting $S = S_{Co} + 3 \times S_{Fe}$ with $g = 2.0$. We cannot find the appropriate model to represent the magnetic susceptibility and evaluate the exchange parameter between low-spin Fe^{III} and high-spin Co^{II} centers.[23,18c]

In the M versus H/T plot, the nonsuperposition of the lines in different magnetic fields is observed (Figure 7), suggesting the existence of zero-field splitting in complexes **2** and **5**. With the spin ground state $S = 2$, fits of the magnetization data using ANISOFIT[22] for $T \leq 5$ K and $H \geq 1$ T afforded $D = -2.36$ and -3.15 cm^{-1} and $g = 2.64$ and 2.77 for **2** and **5**, respectively. Irrespective of the reliability in establishing the sign of D, the best fits

(23) (a) Lescouëzec, R.; Vaissermann, J.; Ruiz-Pérez, C.; Lloret, F.; Carrasco, R.; Julve, M.; Verdaguer, M.; Dromzee, Y.; Gatteschi, D.; Wernsdorfer, W. *Angew. Chem., Int. Ed.* **2003**, *42*, 1483. (b) Toma, L. M.; Lescouëzec, R.; Lloret, F.; Julve, M.; Vaissermann, J.; Verdaguer, M. *Chem. Commun.* **2003**, 1850.

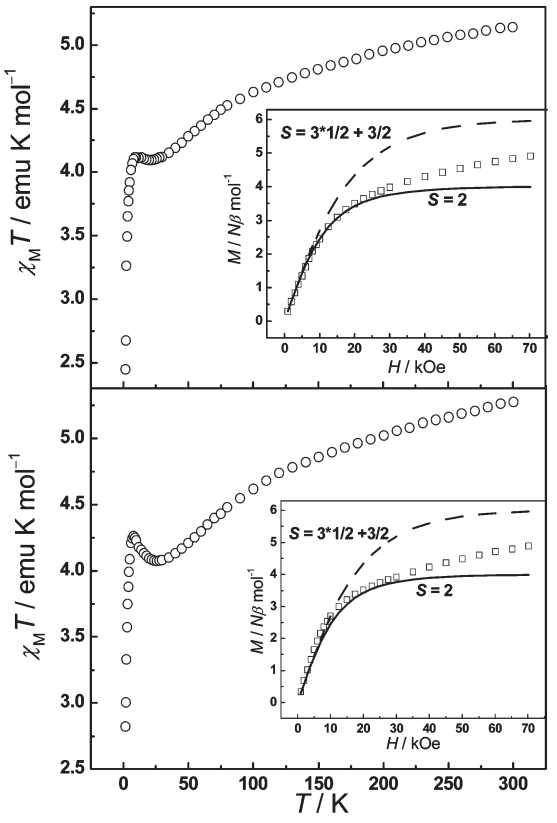

Figure 6. Plots of $\chi_M T$ versus T for **2** (up) and **5** (bottom) at a field of 2 KOe. The insets show magnetization versus field up to $H = 70$ kOe at 1.8 K for **2** (up) and **5** (bottom); the lines represent the Brillouin function that corresponds to noninteracting $S = 3 \times S_{Fe}^{III} + S_{Co}^{II}$ (dotted) and $S = 2$ (solid) with $g = 2.0$.

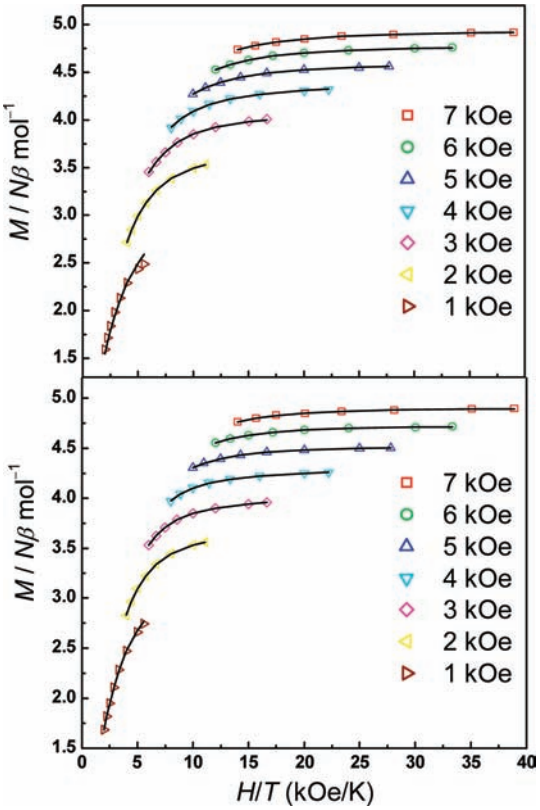

Figure 7. Plots of magnetization vs H/T for **2** (up) and **5** (bottom) between 1.8 and 5 K. Solid lines represent the best fits to the data.

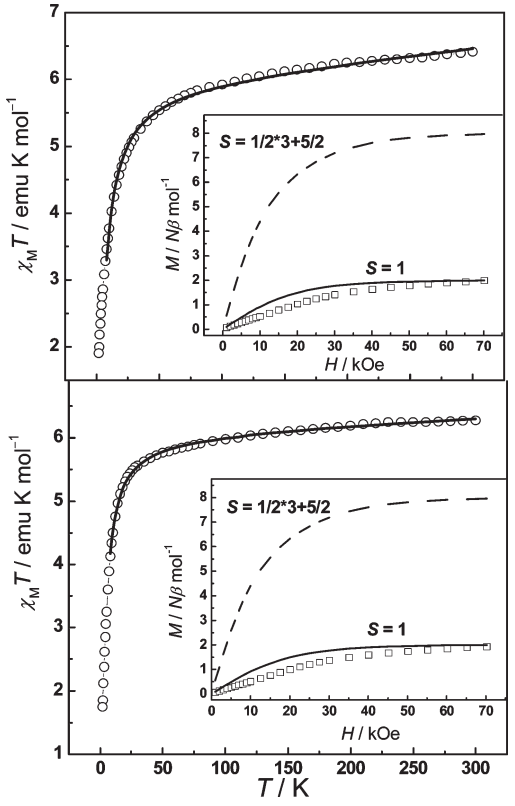

Figure 8. Plots of $\chi_M T$ versus T for **3** (up) and **6** (bottom) at a field of 2 KOe. Solid lines represent the best fitting of the data. The insets show magnetization versus field up to $H = 70$ kOe at 1.8 K for **3** (up) and **6** (bottom); the lines represent the Brillouin function that corresponds to noninteracting $S = 3 \times S_{Fe}^{III} + S_{Mn}^{II}$ (dotted) and $S = 1$ (solid) with $g = 2.0$.

indicate large magnetic anisotropies in both compounds. The g and D values are comparable to the reported cyano-bridged cluster containing Fe^{III} and Co^{II} ions.[8e,16a] The absence of a χ_M'' signal suggests a lack of SMM behavior above 1.8 K for **2** and **5**.

The temperature dependence of susceptibility for **3** and **6** in the form of $\chi_M T$ versus T at 2 kOe is shown in Figure 8. At room temperature, the $\chi_M T$ value is 6.41 emu K mol^{-1} for **3** and 6.27 emu K mol^{-1} for **6**. In **3** and **6**, the carbon-bound cyanides in each T-shaped Fe_3Mn fragment give rise to low-spin Fe^{III} ($S = 1/2$) centers, which are expected to exhibit orbital contributions to the magnetic moment.[19] Assuming that the Mn^{II} centers in **3** and **6** are high-spin with $g_{Mn} = 2$, the magnetic anisotropy of the low-spin Fe^{III} centers present in **3** and **6** can be approximated from $\chi_M T$ data. The calculated g_{Fe} values are ca. 2.69 and 2.60 for **3** and **6**, respectively, which are comparable with the value of $(Bu_4N)[(Tp^{4Bo})Fe(CN)_3]$. Between 300 and 30 K, the $\chi_M T$ values gradually decrease and then do so more abruptly below ca. 10 K, reaching a minimum value of 1.90 and 1.74 emu K mol^{-1} at 1.8 K for **3** and **6**, respectively. It indicates that the Fe^{III} and Mn^{II} centers couple antiferromagnetically. The field-dependent magnetization of **3** and **6** with ca. $M = 1.98$ Nβ mol^{-1} at 7 T has a value of the magnetization expected for an antiferromagnetically coupled $Fe_3^{III}Mn^{II}$ unit. The comparison between calculations based on the Brillouin function and the observed curves is shown in the inset of Figure 8.

An approximate isotropic Hamiltonian similar to that for **1** is used to simulate the magnetic susceptibilities of **3** and **6**, $\hat{H} = -2J\hat{S}_{Mn1}(\hat{S}_{Fe1} + \hat{S}_{Fe2} + \hat{S}_{Fe3})$, and the Van Vleck expression can be written as eq 2:

$$\chi_M = \frac{2Ng^2\beta^2}{kT}\frac{A}{B} \quad (2)$$

$$A = 1 + 5\exp(4J/kT) + 14\exp(10J/kT) + 30\exp(18J/kT) + 10\exp(7J/kT) + 28\exp(13J/kT)$$

$$B = 3 + 5\exp(4J/kT) + 7\exp(10J/kT) + 9\exp(18J/kT) + 10\exp(7J/kT) + 14\exp(13J/kT)$$

The magnetic susceptibilities above 7 K of **3** and **6** were simulated, giving the best fit with parameters $g = 2.13$ and 2.14, $J = -1.21$ and -0.77 cm^{-1}, TIP $= 2.0 \times 10^{-3}$ and 1.0×10^{-3} emu/mol, and $R = 2.5 \times 10^{-3}$ and 5.7×10^{-4}. Simulations of the low-field magnetization versus magnetic field plot at 1.8 K using the same model afforded g values of 1.96 and 1.98 and J values of -1.43 and -1.18 cm^{-1} for **3** and **6**, respectively (see the Supporting Information, Figures S4 and S5). The sign and relative magnitudes of exchange parameters in **3** and **6** are comparable to those of similar clusters: $\{[(Tp^*)Fe(CN)_3Mn(DMF)_4]_2[OTf]_2\}\cdot 2DMF$,[16a] $[(Tp)_2Fe_2(CN)_6Mn(CH_3OH)_4]\cdot 2CH_3OH$,[24a] and $[Fe(pcq)(CN)_3]_2[Mn(CH_3OH)_2(H_2O)_2]\cdot 2H_2O$.[24b]

In summary, a new family of cyano-bridged polynuclear clusters has been synthesized and structurally characterized. These complexes consist of two symmetry-related T-shaped $Fe_3^{III}M^{II}$ (M = Cu, Co, Mn) subunits linked by two Na^+ cations. Each polynuclear cluster strongly interacts with 12 adjacent such units through face-to-face $\pi-\pi$ stacking interactions, leading to a novel 12-connected 3D supramolecular framework. The strategy introducing a weak noncovalent functional group, such as Tp^{4Bo} with an indazole group, which we used here, is perhaps an alternative approach to organizing high-spin clusters with aromatic $\pi-\pi$ stacking interactions.

Acknowledgment. This work was supported by the National Science Fund for Distinguished Young Scholars (20725104), the Major State Basic Research Development Program (2006CB806104 and 2007CB925100), and the National Natural Science Foundation of China (20721002). The authors are very grateful to Prof. You Song and Dr. Tian-Wei Wang for helpful discussions and experimental assistance and a reviewer for invaluable comments on the analyses of magnetic data.

Supporting Information Available: X-ray crystallographic files in CIF format for **1**−**6**, structural figures and additional bond lengths and angles. This material is available free of charge via the Internet at http://pubs.acs.org.

(24) (a) Wang, S.; Zuo, J.-L.; Zhou, H.-C.; Song, Y.; Gao, S.; You, X.-Z. *Eur. J. Inorg. Chem.* **2004**, 3681. (b) Ni, Z.-H.; Kou, H.-Z.; Zhang, L.-F.; Ni, W.-W.; Jiang, Y.-B.; Cui, A.-L.; Ribas, J.; Sato, O. *Inorg. Chem.* **2005**, *44*, 9631.